μ_{-3} = dimensionless group, defined by Equation (54)
$\phi(t)$ = surface age distribution function

LITERATURE CITED

1. Danckwerts, P. V., and A. M. Kennedy, *Chem. Eng. Sci.*, **8**, 201 (1958).
2. Danckwerts, P. V., *Trans. Faraday Soc.*, **46**, 300 (1950).
3. ———, *Ind. Eng. Chem.*, **43**, 1460 (1951).
4. ———, *Trans. Faraday Soc.*, **47**, 1014 (1951).
5. ———, and A. M. Kennedy, *Trans. Inst. Chem. Engrs.*, **32**, S49 (1954).
6. ———, *A.I.Ch.E. J.*, **1**, 456 (1955).
7. Dobbins, W. E., "Biological Treatment of Sewage and Industrial Wastes," J. McCabe and W. W. Eckenfelder, Jr., Eds., Vol. 1, p. 141, Reinhold, New York (1955).
8. Harriott, P., *Chem. Eng. Sci.*, **17**, 149 (1962).
9. Hatta, Shinoji, *Tohoku Imperial Univ. Tech. Repts.*, **10**, 119 (1932).
10. ———, *ibid.*, **8**, 1 (1928-29).
11. ———, *New. Chem. Eng. Ser., Ni Kan Ind. News (Japan)*, VIII-4 (1957).
12. Higbie, Ralph, *Trans. Am. Inst. Chem. Engrs.*, **31**, 365 (1935).
13. Huang, C. J., and C. J. Hsu, paper presented at Am. Chem. Soc. 138th Natl. Meeting, New York (1960).
14. Huang, C. J., and C. H. Kuo, *A.I.Ch.E. J.*, **9**, 161 (1963).
15. Johnson, A. I., and C. J. Huang, *ibid.*, **2**, 412 (1956).
16. Kishinevskii, M. Kh., and A. V. Pamfilov, *Zh. Prikldnai Khimii*, **22**, 1173 (1949).
17. Kishinevskii, M. Kh., *Zh. Prikldnai*, **24**, 542 (1951).
18. ———, *ibid.*, **27**, 382 (1954).
19. Lewis, W. K., and W. G. Whitman, *Ind. Eng. Chem.*, **16**, 1215 (1924).
20. Olander, D. R., *A.I.Ch.E. J.*, **6**, 233 (1960).
21. Onda, K., E. Sada, and H. Takeuchi, *Chem. Eng. (Japan)*, **26**, 984 (1962).
22. Peaceman, D. W., Sc.D. thesis, Massachusetts Inst. Technol., Cambridge, Massachusetts (1951).
23. Perry, R. H., and R. L. Pigford, *Ind. Eng. Chem.*, **45**, 1247 (1953).
24. Roper, G. H., T. F. Hatch, and R. L. Pigford, *Ind. Eng. Chem. Fundamentals*, **1**, 144 (1962).
25. Toor, H. L., and S. H. Chiang, *A.I.Ch.E. J.*, **5**, 339 (1959).
26. Toor, H. L., and J. Marchello, *ibid.*, 4, 97 (1958).
27. Van Krevelen, D. W., and P. J. Hoftijer, *Chem. Eng. Progr.*, **44**, 529 (1948).
28. ———, *Rec. Trav. Chim.*, **67**, 583 (1948).
29. ———, *Trans. Inst. Chem. Eng.*, **32**, S60 (1954).
30. Whitman, W. G., *Chem. Met. Eng.*, **29**, 166 (1933).

Manuscript received October 7, 1964; revision received May 14, 1965; paper accepted May 17, 1965. Paper presented at A.I.Ch.E. San Francisco meeting.

Falling Cylinder Viscometer for Non-Newtonian Fluids

EDWARD ASHARE, R. BYRON BIRD
University of Wisconsin, Madison, Wisconsin

and JAIME A. LESCARBOURA
University of Kansas, Lawrence, Kansas

It is shown how previous analyses of the falling cylinder viscometer for Newtonian fluids can be extended to non-Newtonian fluids. Specific relations are given for the velocity of descent for several simple non-Newtonian viscosity functions. A differentiation procedure is presented whereby the non-Newtonian viscosity for a fluid can be deduced from velocity of fall measurements. In the course of the development, some useful approximate expressions for axial non-Newtonian flow in annuli are developed. Finally, a comparison of the Ellis and power law models is made by an analysis of the axial annular flow data of Frederickson and of McEachern.

The falling cylinder viscometer consists of a long cylindrical container filled with fluid in which a fairly tight-fitting cylindrical slug is allowed to fall under the influence of gravity (see Figure 1). As the cylinder falls, the fluid flows up through the narrow annular slit formed by the cylindrical tube and the falling cylinder. One can measure the rate of steady state descent of the cylinder, and thereby obtain viscometric information. Possible applications of such a device are in: (1) high-pressure measurements, where the sample must be contained in a tight, sturdy cylindrical tube; and (2) biological measurements, where the sample must have minimum contact with the atmosphere.

This system has already been studied for Newtonian fluids. Apparently the earliest analysis was that of Lawaczeck (6), who assumed that the velocity profile in the

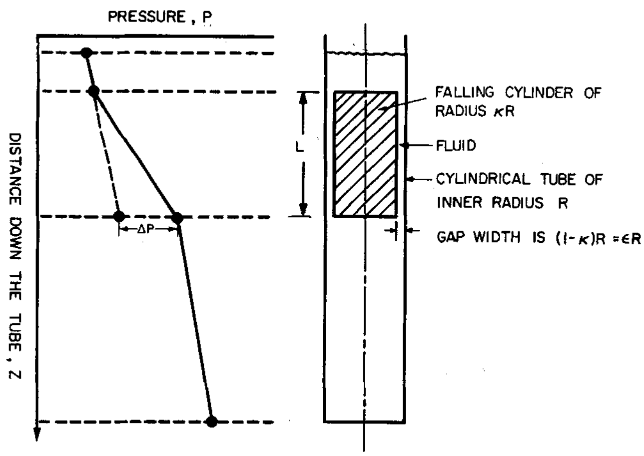

Fig. 1. Schematic diagram of falling cylinder viscometer showing pressure distribution in the fluid.

annular slit could be taken to be nearly the same as that for flow in a *plane* slit with *fixed* walls. These assumptions were not made in a later treatment by Lohrenz, Swift, and Kurata (8), who obtained an expression for the rate of descent of the cylinder and further discussed problems involved in a practical viscometer design.

In the following treatment the possibility that the falling cylinder instrument can be used for non-Newtonian fluids is explored. Initially, it is assumed that: (1) the annular slit is so small that the plane slit approximation is valid, and (2) the falling cylinder moves downward so slowly that, in solving the fluid equations of motion, one can use the approximate boundary condition that the fluid velocity at the falling cylinder surface is zero. Correction factors are then derived to correct for each of these assumptions. Specifically, the power law and Ellis models are used for simple shear flow with $v_z = v_z(x)$, $v_x = v_y = 0$; these models are written thus

Power law model:

$$\tau_{xz} = -m \left| \frac{dv_z}{dx} \right|^{n-1} \frac{dv_z}{dx} \qquad (1)$$

Ellis fluid model:

$$\frac{dv_z}{dx} = -\frac{1}{\eta_0}\left[1 + \left| \frac{\tau_{xz}}{\tau_{1/2}} \right|^{\alpha-1} \right] \tau_{xz} \qquad (2)$$

Finally, we conclude by giving a differentiation method, which provides the shear-stress vs. velocity-gradient curve for any fluid.

Empirical functions of the types shown in Equations (1) and (2) have been shown to be useful in a wide variety of applications. Apparently the constants in Equation (2) are applicable in dimensional analysis of complex flow systems, including those in which viscoelastic phenomena are important (*1*).

It is believed that the falling cylinder system offers greater potential as a device for studying non-Newtonian materials than does the rolling-ball viscometer. For Newtonian fluids Lewis (7) developed an analysis of the rolling-ball viscometer; Bird and Turian extended his work to the power law model (3). Certain aspects of these solutions were helpful in developing the following treatment for the falling cylinder viscometer.

EQUATIONS DESCRIBING THE FALLING CYLINDER

The equations needed to describe the viscometer in Figure 1 are a force balance on the falling cylinder, a statement of conservation of mass for the fluid, and a rheological equation. Our aim is to obtain an equation for the velocity of descent of the falling cylinder.

A *force balance* on the falling cylinder in Figure 1 contains several contributions: (1) force of gravity (acting downward); (2) force due to the pressure difference in excess of the hydrostatic pressure difference as shown in Figure 1 (acting upward); and (3) force of the viscous fluid streaming through the annular slit (acting upward). In computing (3) it will be assumed that the ratio $(L/\epsilon R)$ is sufficiently great that end effects can be neglected; it is also assumed that the falling cylinder is equipped with fins to keep it centered.

The forces listed above, divided by the falling cylinder volume, are given by

$$F_{\text{grav}} = (\rho_0 - \rho) g \qquad (3)$$

$$F_{\text{press}} = (\Delta p / L) \qquad (4)$$

$$F_{\text{visc}} = 2\tau_w / (1-\epsilon) R \qquad (5)$$

in which τ_w is the shear stress at the wall of the falling cylinder. When the falling cylinder attains steady state, the sum of all these forces must be zero.

$$(\rho_0 - \rho) g = \frac{\Delta p}{L} + \frac{2\tau_w}{(1-\epsilon)R} \qquad (6)$$

A *mass balance* on the fluid states that the volume of fluid displaced by the falling cylinder equals the volume of fluid flowing upward in the annular slit.

$$\pi(1-\epsilon)^2 R^2 \, v_0 = [\pi R^2 - \pi(1-\epsilon)^2 R^2] \langle v_z \rangle \qquad (7)$$

Equation (7) may be solved for v_0 to give

$$v_0 = \frac{2\epsilon[1 - \tfrac{1}{2}(\epsilon)]}{(1-\epsilon)^2} \langle v_z \rangle \qquad (8)$$

A *rheological equation* gives τ_{xz} in terms of dv_z/dx or vice versa, and examples of such relations have been given in Equations (1) and (2). Once such a relation is specified, then one can find two functions:

$$\tau_w = f_1(\Delta p) \qquad (9)$$

$$\langle v_z \rangle = f_2(\Delta p) \qquad (10)$$

by elementary hydrodynamics.

The *velocity of descent* of the falling cylinder is then obtained by solving Equations (6), (8), (9), and (10) by eliminating τ_w, $\langle v_z \rangle$, and Δp.

SOLUTION NEGLECTING CURVATURE AND MOVING WALL BOUNDARY CONDITION

If the annular slit width is vanishingly small, it is possible to assume that the slit can be represented by two parallel planes; it is also possible to neglect the small falling cylinder velocity in writing down the boundary condition on the velocity profile at $x = -\tfrac{1}{2}(\epsilon R)$ (see Figure 2*a*). For this degree of approximation (see reference 2, p. 62, Equation 2.E-1)

$$\tau_w{}^0 = \frac{\Delta p}{L} [\tfrac{1}{2}(\epsilon R)] \qquad (11)$$

$$\langle v_z \rangle^0 = \frac{1}{\tfrac{1}{2}(\epsilon R)} \int_0^{1/2(\epsilon R)} v_z dx \qquad (12)$$

where the superscript 0 denotes the zeroeth degree of approximation. Equation (11) is valid for any rheological model; however, Equation (12) depends on the choice of model, and can be rewritten as [see reference 2, p. 68, Prob. 2.0(b)]

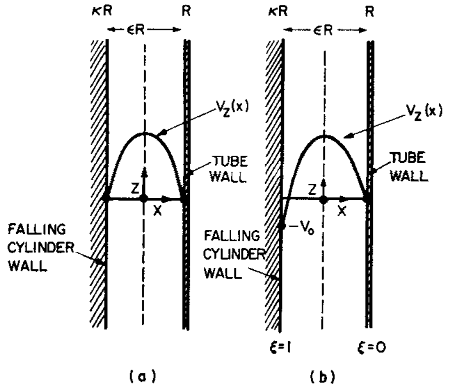

Fig. 2. Coordinate system for viscous flow in thin annular slit between the tube wall and the falling cylinder, assuming slit can be regarded as a plane slit. (*a*) Velocity profile, assuming falling cylinder velocity v_0 is so small that it can be neglected with respect to $\langle v_z \rangle$. (*b*) Velocity profile, with v_0 not assumed negligible.

$$\langle v_z \rangle^0 = \frac{[\frac{1}{2}(\epsilon R)]}{\tau_w^{0^2}} \int_0^{\tau_w^0} \left(-\frac{dv_z}{dx}\right) \tau_{xz}\, d\tau_{xz} \qquad (13)$$

Combination of Equations (6), (8), (11), and (13) then gives

$$(v_0)^0 = \frac{4}{(\rho_0 - \rho)^2 g^2 R} \, \frac{\left(1 - \frac{\epsilon}{2}\right)}{(1-\epsilon)^4} \int_0^{1/2(\epsilon R)(1-\epsilon)(\rho_0 - \rho) g} (-dv_z/dx) \tau_{xz}\, d\tau_{xz} \qquad (14)$$

which can be evaluated by using some specific relation for dv_z/dx as a function of τ_{xz}.

The corrections to Equations (11) and (12) for curvature (c) and for the moving wall condition (m) will be small. Hence, we introduce multiplicative factors in this manner:

$$\tau_w = \tau_w^0 \psi_{\tau c} \psi_{\tau m} = \tau_w^0 \psi_\tau \qquad (15)$$

$$\langle v_z \rangle = \langle v_z \rangle^0 \psi_{vc} \psi_{vm} = \langle v_z \rangle^0 \psi_v \qquad (16)$$

The final expressions for v_0 can then be obtained by combining Equations (6), (8), (11), (12), (15), and (16). We now turn to the calculation of the combined correction factors ψ_v and ψ_τ, which may be developed as power series in ϵ.

CORRECTION TO THE AVERAGE VELOCITY

First we find the correction for the Newtonian fluid, and then we show that the same correction seems to be applicable to non-Newtonian fluids.

For the Newtonian fluid of viscosity μ, the average velocity in a plane slit of thickness $(1 - \kappa)R = \epsilon R$ is (see reference 2, p. 62, Prob. 2E, Ans.)

$$\langle v_z \rangle_{\text{slit}} = \frac{\Delta p R^2}{3 \mu L} \left(\frac{1-\kappa}{2}\right)^2 \qquad (17)$$

Also, the flow in an annulus of radii κR and R with the inner wall moving (see Figure 2*b*) is the same as §2.4 in reference 2, except that the boundary condition at $r = \kappa R$ is $v_z = -v_0$. Hence, the velocity distribution becomes

$$v_z = \frac{\Delta p R^2}{4 \mu L} \left[(1 - \zeta^2) - (1 - \kappa^2) \frac{\ln \zeta}{\ln \kappa} \right] - v_0 \frac{\ln \zeta}{\ln \kappa} \qquad (18)$$

where $\zeta = r/R$. The average velocity is found by integrating Equation (18) across the annular slit; and if Equation (8) is then used

$$\langle v_z \rangle_{\text{Fall. Cyl.}} = -\frac{\Delta p (\kappa R)^2}{4 \mu L} \left[\frac{1 + \kappa^2}{1 - \kappa^2} \ln \kappa + 1 \right] \qquad (19)$$

The velocity correction ψ_0 is then found by dividing Equation (19) by Equation (17):

$$\psi_v = \frac{\langle v_z \rangle_{\text{Fall. Cyl.}}}{\langle v_z \rangle_{\text{slit}}} = 1 - \epsilon - \frac{3}{20}\epsilon^2 + \frac{1}{35}\epsilon^4 + \ldots \qquad (20)$$

This is the final expression for the correction to $\langle v_z \rangle$ for Newtonian fluids. Note that for $\epsilon \leqq 0.5$, no terms of order higher than ϵ^2 need be retained. Next it is desired to justify the use of the same correction factor for non-Newtonian fluids. To do this ψ_v is broken up into its components, ψ_{vc} and ψ_{vm}, and each of them is examined separately.

(1) First we consider ψ_{vc}. For Newtonian fluids, the average velocity in an annulus is (see reference 2, p. 53, Equation 2.4-15)

$$\langle v_z \rangle_{\text{Ann}} = \frac{\Delta p R^2}{8 \mu L} \left(\frac{1 - \kappa^4}{1 - \kappa^2} + \frac{1 - \kappa^2}{\ln \kappa} \right) \qquad (21)$$

The correction factor ψ_{vc} is obtained by dividing Equation (21) by (17) (see reference 2, pp. 62-63. Prob. 2.F).

$$\psi_{vc} = 1 + \frac{1}{60}\epsilon^2 + \frac{1}{60}\epsilon^3 + \frac{37}{2520}\epsilon^4 + \ldots \qquad (22)$$

Note that there is no term in ϵ and that the coefficients of higher order terms are small. Hence, for small values of ϵ, this correction will not be of much importance.

For non-Newtonian fluids Equation (22) seems to be valid in our range of interest. In order to prove this we use Fredrickson and Bird's results (5) for power law fluids:

$$\langle v_z \rangle_{\text{Ann}} = \left(\frac{\Delta p \epsilon R}{2 m L}\right)^s \frac{\epsilon R}{2(s+2)} \, \frac{\Upsilon(s, \kappa)}{[1 - \frac{1}{2}(\epsilon)]} \qquad (23)$$

$$\langle v_z \rangle_{\text{slit}} = \left(\frac{\Delta p \epsilon R}{2 m L}\right)^s \frac{\epsilon R}{2(s+2)} \qquad (24)$$

in which $s = 1/n$ and $\Upsilon(s, \kappa)$ is a tabulated function of Fredrickson and Bird. Hence

$$\psi_{vc} = \frac{\Upsilon(s, \kappa)}{[1 - \frac{1}{2}(\epsilon)]} \quad \text{(power law)} \qquad (25)$$

TABLE 1. PERCENT DIFFERENCE BETWEEN ψ_{vc} IN EQUATIONS (22) AND (25)

	κ			
s	0.6	0.7	0.8	0.9
1	0.06	0.02	0.01	0.00
2	0.46	0.21	0.09	0.02
3	0.67	0.36	0.17	0.04
4	0.99	0.42	0.22	0.06

$$\%\ \text{Diff} = \frac{\psi_{vc}\ \text{Eq. (25)} - \psi_{vc}\ \text{Eq. (22)}}{\psi_{vc}\ \text{Eq. (22)}} \times 100$$

In Table 1 is shown the percent difference between ψ_{vo} as calculated by Equation (22) and Equation (25).

A further proof of the validity of Equation (22) can be shown by using McEachern's (*11*) recently calculated results for Ellis fluid flow in annuli. He tabulated values of $\langle v_z \rangle_{\text{Ann}} \; \epsilon[1 - \frac{1}{2}(\epsilon)]\eta_0/R\tau_{1/2}$ as a function of $\Delta pR/2L\,\tau_{1/2}$, α, and κ, using an exact solution for annular flow given by

$$\frac{\langle v_z \rangle_{\text{Ann}}\epsilon[1 - \frac{1}{2}(\epsilon)]\eta_0}{R\tau_{1/2}} = \frac{\Delta pR}{2L\tau_{1/2}} \int_\kappa^1 \left(\frac{\lambda^2}{\xi} - \xi\right)^2 \xi \, d\xi + \left(\frac{\Delta pR}{2L\tau_{1/2}}\right)^\alpha \int_\kappa^1 \left|\frac{\lambda^2}{\xi} - \xi\right|^{\alpha+1} \xi \, d\xi \qquad (26)$$

The approximate solution for Ellis fluid flow in a slit is given by

$$\frac{\langle v_z \rangle_{\text{Slit}}\epsilon[1 - \frac{1}{2}(\epsilon)]\eta_0}{R\tau_{1/2}} = \epsilon^2[1 - \tfrac{1}{2}(\epsilon)] \left[\frac{1}{3}\left(\frac{\Delta pR\epsilon}{2L\tau_{1/2}}\right) + \frac{1}{\alpha + 2}\left(\frac{\Delta pR\epsilon}{2L\tau_{1/2}}\right)^\alpha\right] \qquad (27)$$

and

$$\psi_{vc} = \frac{\langle v_z \rangle_{\text{Ann}} \text{ (Eq. 26)}}{\langle v_z \rangle_{\text{Slit}} \text{ (Eq. 27)}} \qquad \text{(Ellis model)} \qquad (28)$$

In Table 2 is given the percent difference between ψ_{vc} as calculated by Equation (22) and Equation (28).

It is interesting to note that Tables 1 and 2 suggest that non-Newtonian annular flow can often be approximated very well by slit flow if one is interested in the average velocity only. (In the appendix experimental data are used to show that this approximation is indeed applicable.) For the problem at hand the error will be less than 1% for $s \leq 4$ and $\kappa > 0.6$. Hence, Equation (22) can be applied with confidence in the viscometer analysis.

(2) Next we consider the factor ψ_{vm}. For the Newtonian fluid this moving wall correction is found by dividing Equation (19) by Equation (21).

$$\psi_{vm} = \frac{\langle v_z \rangle_{\text{Fall. Cyl}}}{\langle v_z \rangle_{\text{Ann}}} = 1 - \epsilon - \frac{1}{6}\epsilon^2 + \frac{1}{30}\epsilon^4 + \ldots \qquad (29)$$

It should be noted that the product $\psi_{vm} \cdot \psi_{vo}$ does indeed give ψ_v.

Next we would like to justify the use of Equation (29) for non-Newtonian fluids. However, since an analytical solution for $\langle v \rangle_{\text{Fall. Cyl.}}$ is not available for any non-Newtonian model, we content ourselves by considering the analogous plane slit problem; that is, we compute ψ_{vm} for the limiting case of small ϵ. For this purpose it is convenient to introduce a new coordinate ξ, which is zero at $x = -\frac{1}{2}(\epsilon R)$ and is unity at $x = -\frac{1}{2}(\epsilon R)$; the location of the velocity maximum is then given as $\xi = \lambda$ (see Figures 2*a* and 2*b*).

We now make the calculation for the power law model. The equation of motion gives

$$\tau_{xz} = \left(\frac{\Delta p\epsilon R}{L}\right)(\xi - \lambda) \qquad (30)$$

and the rheological model is

$$\tau_{xz} = \begin{cases} -m(dv_z/dx)^n & \xi < \lambda \\ +m(-dv_z/dx)^n & \xi > \lambda \end{cases} \qquad (31)$$

TABLE 2. PERCENT DIFFERENCE BETWEEN ψ_{vc} IN EQUATIONS (22) AND (28)

	κ				
a	0.5	0.6	0.7	0.8	0.9
1.5	0.74	0.35	0.15	0.10	0.00
2.0	1.04	0.54	0.25	0.10	0.10
2.5	1.35	0.74	0.30	0.10	0.05
3.0	1.60	0.88	0.39	0.12	—
4.0	2.09	1.07	0.68	0.42	—

$$\%\text{ diff} = \frac{\psi_{vc}\text{ Eq. (28)} - \psi_{vc}\text{ Eq. (22)}}{\psi_{vc}\text{ Eq. (28)}} \times 100$$

Solution for the velocity profiles gives (with $s = 1/n$)

$$v_z = -v_0 + \frac{\epsilon R}{s+1}\left(\frac{\Delta p\epsilon R}{mL}\right)^s [(1-\lambda)^{s+1} - (\xi - \lambda)^{s+1}] \quad \xi > \lambda \qquad (32)$$

$$v_z = \frac{\epsilon R}{s+1}\left(\frac{\Delta p\epsilon R}{mL}\right)^s [\lambda^{s+1} - (\lambda - \xi^{s+1}] \quad \xi < \lambda \qquad (33)$$

We now equate these expressions at $\xi = \lambda$ and set

$$\phi_0 \equiv \frac{v_0}{\dfrac{\epsilon R}{s+1}\left(\dfrac{\Delta p\epsilon R}{mL}\right)^s} \qquad (34)$$

Then

$$-\phi_0 + (1-\lambda)^{s+1} = \lambda^{s+1} \qquad (35)$$

which determines $\lambda = \lambda(\phi_0, s)$. We assume that λ can be written as a power series in ϕ_0 and thereby solve Equation (35) to obtain

$$\lambda = \frac{1}{2}\left[1 - \frac{2^s}{s+1}\phi_0 + \frac{2^{3s}}{3!}\frac{s(s-1)}{(s+1)^3}\phi_0^3 + \ldots\right] \qquad (36)$$

Clearly, when $v_0 \to 0$, then $\lambda \to \frac{1}{2}$, as it should in a slit.

From Equations (32), (33), and (36) one may calculate $\langle v_z \rangle$ for the moving wall slit and the stationary slit and then get their ratio. When an expansion in powers of ϕ_0 is made, one obtains

$$\psi_{vm} = \frac{\langle v_z \rangle_{\text{Mov. Slit}}}{\langle v_z \rangle_{\text{Fixed Slit}}} = 1 - \left[2^s\left(\frac{s+2}{s+1}\right)\phi_0\right] + \frac{(s-1)}{2(s+2)}\left[2^s\left(\frac{s+2}{s+1}\right)\phi_0\right]^2 + O(\phi_0^4) + \ldots \qquad (37)$$

Next, Equations (34), (24), and (8) can be used to rewrite the result in terms of ϵ:

$$\psi_{vm} = 1 - \epsilon - \frac{3}{2}\left[\frac{2s+7}{3(s+2)}\right]\epsilon^2 + O(\epsilon^3) + \ldots \qquad (38)$$

Note that the term in brackets is a slowly varying function of s, going from unity for Newtonian fluids ($s = 1$) to 5/6 for $s = 4$ (quite non-Newtonian). Hence, Equation (38) demonstrates that for flat plates, the term of order ϵ is independent of the fluid, and that the term in ϵ^2 depends only slightly on the nature of the fluid. (A similar calculation for the Ellis model leads to essentially the same conclusions.)

Finally, we can infer that Equation (29) will probably be suitable for non-Newtonian fluids up through the term in ϵ and will be only slightly in error in terms of order ϵ^2 and higher.

CORRECTIONS TO THE WALL SHEAR STRESS

For the Newtonian fluid the shear stress on the falling cylinder can be calculated both for the true situation and for the plane slit approximation. If we combine Equations (18), (8), and (19), the velocity distribution for the falling cylinder system becomes

$$v_z = \frac{\Delta p R^2}{4\mu L}\,[(1-\zeta^2) + (1+\kappa^2)\ln\zeta] \qquad (39)$$

Then

$$\tau_w = -\tau_{rz}\Big|_{r=\kappa R} = \frac{\mu}{R}\,\frac{dv_z}{d\zeta}\Big|_{\zeta=\kappa} \qquad (40)$$

or

$$(\tau_w)_{\text{Fall. Cyl.}} = \frac{\Delta p R\epsilon}{2L}\left(\frac{[1-\tfrac{1}{2}(\epsilon)]}{1-\epsilon}\right) \qquad (41)$$

For the plane slit approximation

$$(\tau_w)_{\text{Slit}} = \frac{\Delta p R\epsilon}{2L} \qquad (42)$$

so that

$$\psi_\tau = \frac{1-\tfrac{1}{2}(\epsilon)}{1-\epsilon} \qquad (43)$$

The individual correction factors are found to be

$$\psi_{\tau c} = 1 + \frac{1}{6}\epsilon + \frac{1}{6}\epsilon^2 + \frac{29}{180}\epsilon^3 + \frac{7}{45}\epsilon^4 + \ldots \qquad (44)$$

$$\psi_{\tau m} = 1 + \frac{1}{3}\epsilon + \frac{5}{18}\epsilon^2 + \frac{32}{135}\epsilon^3 + \frac{83}{405}\epsilon^4 + \ldots \qquad (45)$$

and the product $\psi_{\tau c}\cdot\psi_{\tau m}$ is equal to ψ_τ.

No effort is made to justify the use of Equation (43) for non-Newtonian fluids, inasmuch as the correction ψ_τ turns out to be less important than ψ_v, as will be shown presently.

FINAL RESULTS FOR EMPIRICAL MODELS

We can now combine the preceding results for the Newtonian fluid and two non-Newtonian empirical models of interest. Specifically, for the Newtonian fluid we combine Equations (6), (8), (11), (15), (16), and (17) to obtain

$$v_0 = \frac{2\epsilon[1-\tfrac{1}{2}(\epsilon)]}{(1-\epsilon)^2}\cdot\frac{R^2}{3\mu}\left(\frac{\epsilon}{2}\right)^2\psi_v\cdot\frac{(\rho_0-\rho)g}{1+\dfrac{\epsilon}{1-\epsilon}\psi_\tau} \qquad (46)$$

It should be noted that ψ_v is more important than ψ_τ by one order of magnitude.

For the power law model, we combine Equations (6), (8), (11), (15), (16), and (24) to obtain

$$v_0 = \frac{2\epsilon[1-\tfrac{1}{2}(\epsilon)]}{(1-\epsilon)^2}\cdot\frac{\epsilon R}{2(s+2)}\left(\frac{\epsilon R}{2m}\right)^s\psi_v\cdot\left[\frac{(\rho_0-\rho)g}{1+\dfrac{\epsilon}{1-\epsilon}\psi_\tau}\right]^s \qquad (47)$$

Similarly, for the Ellis model, one obtains

$$v_0 = \frac{2\epsilon[1-\tfrac{1}{2}(\epsilon)]}{(1-\epsilon)^2}\,\frac{\epsilon R\tau_{1/2}}{2\eta_0}\psi_v\left\{\frac{1}{3}\left[\frac{(\rho_0-\rho)g\,\epsilon R}{2\tau_{1/2}\left(1+\dfrac{\epsilon}{1-\epsilon}\psi_\tau\right)}\right] + \frac{1}{\alpha+2}\left[\frac{(\rho_0-\rho)g\,\epsilon R}{2\tau_{1/2}\left(1+\dfrac{\epsilon}{1-\epsilon}\psi_\tau\right)}\right]^\alpha\right\} \qquad (48)$$

From these results and experimental data on v_0 for various $(\rho_0-\rho)$, one should be able to determine the model parameters, provided that the fluids are indeed describable by the model.

For the *power law fluid* a plot of log v_0 vs. log $(\rho_0-\rho)$ should be a straight line of slope s; the parameter m can then be obtained from any pair of v_0 and $(\rho_0-\rho)$ values.

For the *Ellis fluid*, the procedure is more complicated. Equation (48) can be written as

$$\Gamma = \frac{1}{3}T + \frac{1}{\alpha+2}T^\alpha \qquad (49)$$

in which

$$\Gamma = \frac{v_0\eta_0(1-\epsilon)^2}{\epsilon^3 R\tau_{1/2}[1-\tfrac{1}{2}(\epsilon)]\psi_v} \qquad (50)$$

$$T = \frac{(\rho_0-\rho)\,g\,\epsilon\,R}{2\tau_{1/2}\left(1+\dfrac{\epsilon}{1+\epsilon}\psi_\tau\right)} \qquad (51)$$

First a master plot of log Γ vs. log T is made for various values of α (solid curves in the sketch in Figure 3). Next from the experimental data a plot of log v_0 vs. log $(\rho_0-\rho)$ is made on transparent paper (dashed curves in Figure 3). The experimental plot is then slid around on the

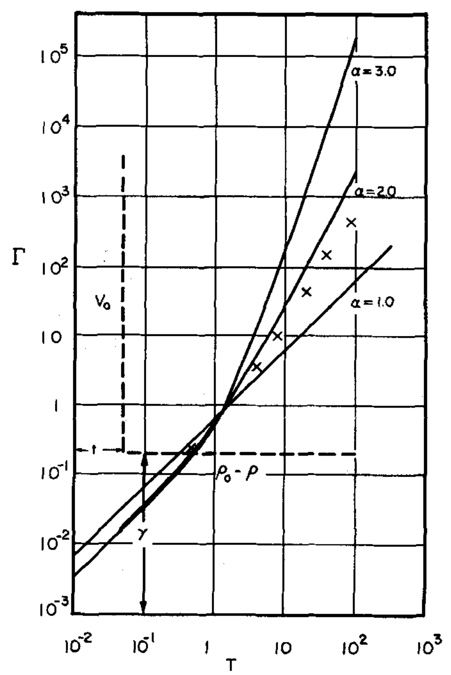

Fig. 3. Sketch showing how to determine Ellis model parameters from falling cylinder viscometer data.

master plot, keeping the axes of both plots parallel, until the data points fall on one of the master curves; this determines α. The displacements t and γ are measured, and from these one obtains $\tau_{1/2}$ and η_0:

$$\tau_{1/2} = \frac{g\epsilon R}{2t\left(1 + \frac{\epsilon}{1-\epsilon}\psi_\tau\right)} \tag{52}$$

$$\eta_0 = \epsilon^2 R \; \tau_{1/2}\gamma \frac{[1 - \frac{1}{2}(\epsilon)]\psi_v}{(1-\epsilon)^2} \tag{53}$$

This procedure enables one to see graphically whether a fluid can indeed be described by the model in question.

DEDUCTION OF RHEOLOGICAL MODEL FROM FALLING CYLINDER DATA

By combining Equations (8), (14), and (16), we obtain the following expression for the rate of descent of the falling cylinder:

$$v_0 = \frac{4}{(\rho_0 - \rho)^2 g^2 R} \frac{\left(1 - \frac{\epsilon}{2}\right)}{(1-\epsilon)^4} \int_0^{1/2(\epsilon R)(1-\epsilon)(\rho_0 - \rho)g} (-dv_z/dx)\, \tau_{xz}\, d\tau_{xz} \cdot \psi_v \tag{54}$$

An expression for ψ_v can be inserted explicitly from Equation (20). When Equation (54) is multiplied by $(\rho_0 - \rho)^2$ and differentiated with respect to $(\rho_0 - \rho)$, one obtains

$$\left(-\frac{dv_z}{dx}\right)_{\text{wall}} = \frac{(1-\epsilon)^2}{[1 - \frac{1}{2}(\epsilon)]\epsilon^2\psi_v} \frac{1}{(\rho_0 - \rho)R} \frac{d}{d(\rho_0 - \rho)} [v_0(\rho_0 - \rho)^2] =$$

$$\left(1 - \tfrac{1}{2}(\epsilon) - \frac{1}{10}\epsilon^2 - \frac{1}{20}\epsilon^3 + \ldots\right) \frac{1}{(\rho_0 - \rho)\,\epsilon^2 R} \frac{d}{d(\rho_0 - \rho)} [v_0(\rho_0 - \rho)^2] \tag{55}$$

This velocity gradient is that at the wall for flow in a plane slit with no motion of the walls. Furthermore, from Equations (6), (11), and (15) we have the analogous expression for the shear stress:

$$(\tau_{xz})_{\text{wall}} = \tfrac{1}{2}(\epsilon R)(\rho_0 - \rho)g \Big/ \left(1 + \frac{\epsilon}{1-\epsilon}\psi_\tau\right) =$$

$$[1 - \epsilon - \tfrac{1}{2}(\epsilon^2) + \tfrac{1}{4}(\epsilon^4) + \ldots]\, \tfrac{1}{2}(\epsilon R)(\rho_0 - \rho)g \tag{56}$$

From Equations (55) and (56) one can then deduce the relationship between τ_{xz} and $(-dv_z/dx)$ by making measurements of v_0 for many values of ρ_0 (for known ρ, ϵ, R, and g). The velocity gradient is obtained by a differentiation procedure in Equation (55) and the shear stress is obtained from the simple formula in Equation (56). These equations can be checked for the simple case of the power law model by substituting Equation (47) into Equation (55); in this way one finds that $(-dv_z/dx) = (\tau_{xz}/m)^s$, which verifies that the levels of approximation in Equations (55) and (56) are consistent.

It, therefore, appears that the falling cylinder viscometer data for non-Newtonian fluids can be interpreted in order to get model constants or to deduce the non-Newtonian viscosity of tht fluid.

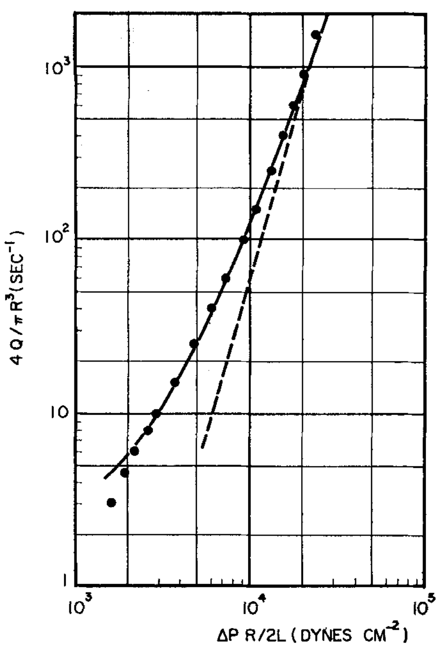

Fig. 4. Volume flow rate of 3.5% CMC-70—medium in annulus (κ = 0.624). Solid curve—Ellis model (α = 3.0, η_0 = 22.7 poises, $\tau_{1/2}$ = 1,520 dynes cm.$^{-2}$). Dashed curve—power law model (n = 0.280, m = 606 dynes cm.$^{-2}$ sec.^{n}). Points—data of Fredrickson (4). (Model parameters obtained from data of Fredrickson.)

ACKNOWLEDGMENT

The authors wish to acknowledge financial assistance provided by National Science Foundation Grant GP-1875. Also, one of the authors (EA) thanks the Standard Oil Company of California for fellowship assistance, and the other (JAL) thanks the Continental Oil Company for financial support. Also, we wish to thank Professor G. W. Swift of the Department of Chemical and Petroleum Engineering at the University of Kansas for helpful comments in connection with extending his earlier work to non-Newtonian fluids.

NOTATION

g = acceleration due to gravity
L = length of falling cylinder
m = power law parameter
n = power law parameter
Q = volume rate of flow
R = radius of outer (stationary) cylinder
s = power law parameter ($s = 1/n$)
T = variable defined by Equation (51)
t = displacement shown in Figure 3
$v_z(x)$ = velocity of fluid in slit at position x
$\langle v_z \rangle$ = average velocity of fluid in slit
v_0 = velocity of falling cylinder
x = distance variable in slit (Figure 2)

Greek Letters

α = Ellis model parameter
Γ = variable defined by Equation (50)
Δp = pressure difference in excess of hydrostatic difference between bottom and top of falling cylinder
γ = displacement shown in Figure 3
ϵ = slit width divided by outer cylinder radius ($\epsilon = 1 - \kappa$)
η_0 = Ellis model parameter; zero shear viscosity

ζ = dimensionless variable, $\zeta = r/R$
κ = ratio of inner cylinder radius to outer cylinder radius
λ = position of maximum velocity in slit
μ = Newtonian viscosity
ξ = dimensionless distance variable in slit (Figure 2)
ρ = fluid density
ρ_0 = falling cylinder density
τ_w = shear stress at falling cylinder surface
τ_{yx} = shear stress of fluid in slit at position x
$\tau_{1/2}$ = Ellis model parameter–shear stress at $\eta = \frac{1}{2}\eta_0$
Υ = function tabulated by Fredrickson and Bird (5)
ϕ_0 = variable defined by Equation (34)
$\psi_v, \psi_{vc}, \psi_{vm}$ = corrections to average velocity in Equation (16)
$\psi_\tau, \psi_{\tau c}, \psi_{\tau m}$ = corrections to wall shear stress in Equation (15)

LITERATURE CITED

1. Bird, R. B., *Chem. Eng. Progr. Symposium Ser. No. 58*, **61**, Chap. 6 (1965).
2. ———, W. E. Stewart, and E. N. Lightfoot, "Transport Phenomena," Wiley, New York (1960); fourth corrected printing (1964).
3. Bird, R. B., and R. M. Turian, *Ind. Eng. Chem. Fundamentals*, **3**, 87 (1964).
4. Frederickson, A. G., Ph.D. thesis, Univ. Wisconsin, Madison, Wisconsin (1959).
5. ———, and R. B. Bird, *Ind. Eng. Chem.*, **50**, 347 (1958); erratum, *Ind. Eng. Chem. Fundamentals*, 3, 383 (1964).
6. Lawaczeck, F., *Z. Ver. Deut. Ing.*, **63**, 677 (1919).
7. Lewis, H. W., *Anal. Chem.*, **25**, 507 (1953).
8. Lohrenz, J., G. W. Swift, and F. Kurata, *A.I.Ch.E. J.*, **6**, 547 (1960); erratum, *ibid.*, **7**, 6S (1961).
9. Matsuhisa, Seikichi, and R. B. Bird, *A.I.Ch.E. J.*, **11**, No. 4, 588-595 (1965).
10. McEachern, D. W., Ph.D. thesis, Univ. Wisconsin, Madison, Wisconsin (1963).
11. ———, paper presented at A.I.Ch.E. Houston meeting (February, 1965).

APPENDIX. ANALYSIS OF AXIAL ANNULAR FLOW DATA

Annular flow data for several aqueous polymer solutions were obtained by Frederickson (*4*) and by McEachern (*10*). They compared plots of $4Q/\pi R^3$ vs. $\Delta pR/2L$ for experimental annular flow data with the following theoretical relation for power law flow in an annulus, given by (*5*).

$$\frac{4Q}{\pi R^3} = \frac{4\epsilon^{s+2}}{s+2}\Upsilon(s,\kappa)\left(\frac{\Delta pR}{2Lm}\right)^s \tag{57}$$

for an annulus made of inner and outer cylinders of radii κR and R, respectively. Power law parameters for the various fluids were obtained from capillary tube viscometric data. The values obtained from Fredrickson's data are given in (*4*), but the values obtained from McEachern's data were obtained by fitting the data as well as possible over the entire shear stress range. (These parameters were reevaluated because McEachern chose his m and n to fit that shear stress range that was the most important for his annular flow experiments, thereby prejudicing the values in favor of a good description of the annular data.)

A theoretical relation for the volume rate of flow of an Ellis fluid in an annulus can be obtained by using the relation for Ellis fluid flow in a slit multiplied by the curvature correction for average flow rate. This results in

$$\frac{4Q}{\pi^3 R} = \frac{4\epsilon^2[1-\frac{1}{2}(\epsilon)]\psi_{vc}\,\tau_{1/2}}{\eta_0}\left[\frac{1}{3}\left(\frac{\Delta pR\epsilon}{2L\tau_{1/2}}\right) + \frac{1}{\alpha+2}\left(\frac{\Delta pR\epsilon}{2L\tau_{1/2}}\right)^\alpha\right] \tag{58}$$

where ψ_{vc} is the function given in Equation 22. Ellis fluid parameters were obtained by a graphical procedure described by Matsuhisa and Bird (9).

The volume flow rates are shown in Figures 4, 5, and 6. The solid curve is the theoretical relation for the Ellis model [Equation (58)], and the dashed curve is the relation for the power law model [Equation (57)]. It can be seen from these plots that the Ellis model curve fits the data better than the power law curve, especially for 3.5% carboxymethyl cellulose (CMC) Figure 4. Also, it is noted that the slit relation for the Ellis model multiplied by the curvature correction to the flow rate is applicable to annular flow.

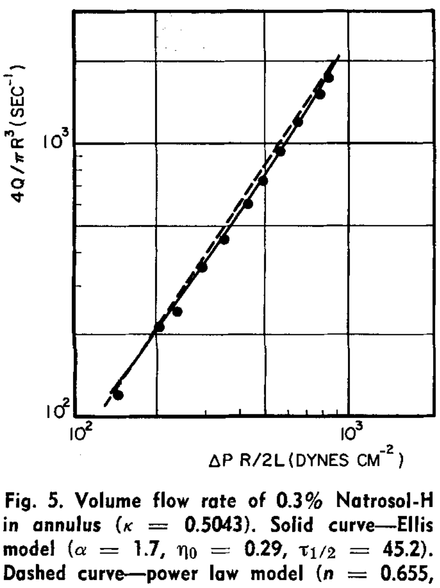

Fig. 5. Volume flow rate of 0.3% Natrosol-H in annulus (κ = 0.5043). Solid curve—Ellis model (α = 1.7, η_0 = 0.29, $\tau_{1/2}$ = 45.2). Dashed curve—power law model (n = 0.655, m = 1.128). Points—data of McEachern (*10*). (Model parameters obtained from data of McEachern.)

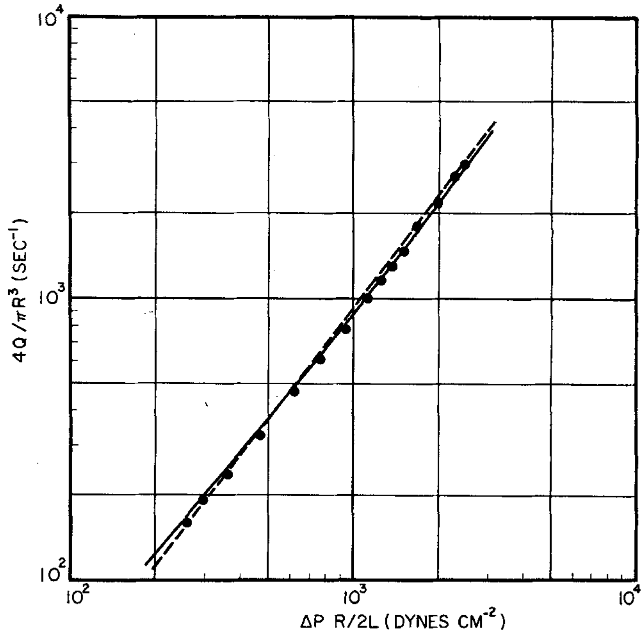

Fig. 6. Volume flow rate of 1.0% Natrosol-G in annulus (κ = 0.5043). Solid curve—Ellis model (α = 1.5, η_0 = 0.31, $\tau_{1/2}$ = 260). Dashed curve—power law model (n = 0.763, m = 0.893). Points—data of McEachern (*10*). (Model parameters obtained from data of McEachern.)

Manuscript received December 11, 1964; revision received May 10, 1965; paper accepted May 13, 1965.